Journal of Palaeosciences 70(2021): 253–265
0031–0174/2021

Centennial to millennial–scale changes in thermocline ventilation in the Arabian Sea: insights from the pteropod preservation record

ARUN DEO SINGH

Micropaleontology and Oceanography Laboratory, Department of Geology, Institute of Science, Banaras Hindu University, Varanasi 221 005, India.
Email: arundeosingh@yahoo.com

ABSTRACT

Singh AD 2021. Centennial to millennial–scale changes in thermocline ventilation in the Arabian Sea: insights from the pteropod preservation record. Journal of Palaeosciences 70(2021): 253–265.

The Arabian Sea hosts one of the three thickest oxygen minimum zones (OMZs) of the world ocean. Mid–depth oxygen depletion profoundly influences the chemistry of thermocline waters (HCO_3^-, CO_3^{2-} and pH), which in turn significantly influences the preservation state of carbonates. The carbonate preservation is primarily controlled by the degree of saturation level of seawater with respect to the calcite and aragonite. The seawater in OMZ is undersaturated with respect to the aragonite (a metastable polymorph of $CaCO_3$). Pteropod test being aragonitic in composition is therefore highly susceptible to the dissolution and dissolves completely below the aragonite compensation depth (ACD). Because of the current condition of intense OMZ due to high primary productivity, enhanced respiration of sinking organic carbon and reduced thermocline circulation; the ACD is shallow, lying in the middle of the OMZ. Hence, preservation record of pteropods in sea–floor sediment archives past changes in thermocline oxygen condition, carbonate chemistry, the ACD and OMZ intensity. High resolution records of various pteropod preservation indices (total pteropod abundance, transparent *Limacina inflata* abundance, fragmentation index) in a sediment core from the lower OMZ of the Indian margin (off Goa) enabled to investigate aragonite preservation/dissolution events and their links with the changes in ACD and OMZ intensity in the eastern Arabian Sea during the last 70 kyr BP. The proxy records reveal centennial to millennial scale changes in aragonite preservation condition in concert with Northern Hemisphere climatic events (Dansgaard–Oeschger (D–O) cycles and Heinrich events). The pteropod preservation spikes apparently correspond to the Northern Hemisphere cold events (D–O stadials and Heinrich events). Whereas, the pteropod tests were either poorly preserved or completely dissolved during the warm phases of D–O cycles (interstadials). The aragonite preservation events are attributed to the low monsoon induced productivity combined with the increased thermocline ventilation by Subantarctic Mode and Antarctic Intermediate Waters (SAMW–AAIW) resulting a weak OMZ and deeper ACD. The novel proxies (abundances of *Globorotalia menardii*, a planktic foraminifera and *Styliola subula*, a pteropod species) are used to gain better insights in to the variability of thermocline ventilation and OMZ intensity through time.

Key–words—Pteropods, Monsoon, ACD, OMZ, Thermocline ventilation, SAMW–AAIW.

INTRODUCTION

IN recent years, there has been a growing interest in investigating perturbations in physico–chemical properties of surface and sub–surface ocean waters due to current scenario of global warming and rising atmospheric CO_2 and its impact on marine biota. Studies have shown that the rising atmospheric CO_2 in recent times has led to increased CO_2 uptake by the oceans resulting in decrease of the seawater pH and as a consequence reduction of carbonate saturation level (e.g., Riebesell *et al.*, 2000; Feely *et al.*, 2004; Sabine *et al.*, 2004; Orr *et al.*, 2005). The oxygen depletion at mid–water depth can potentially expand the oxygen minimum zone in oceans, and that will profoundly impact the biological processes, nutrient cycling, deep ocean biosphere and global climate (Keeling & Garcia, 2002; Stramma *et al.*, 2008). The mid–water oxygen minima also referred as oxygen minimum zone (OMZ) or oxygen–deficient zone (ODZ) develops, where the oxygen consumption exceeds the supply of O_2 within the water column (Olson *et al.*, 1993). The Arabian Sea is one of the few areas in the world hosting well developed OMZ within thermocline between 150 and 1200 m depths (e.g., Altabet *et al.*, 1995). An intensified, perennial OMZ in the Arabian Sea today is attributed to the seasonal monsoon winds induced high primary productivity, high rates of respiration of sinking organic matter in the water column coupled with a poor thermocline ventilation (Schulz *et al.*, 1998; Altabet *et al.*, 2002; Singh *et al.*, 2006; Singh, 2007). Changes in the intensity of the OMZ and its expansion and contraction have significant impact on oceanic nutrient inventory, which in turn influences global productivity and CO_2 sequestration by the biological pump and global climate (Keeling & Garcia, 2002; Stramma *et al.*, 2008). Therefore, it is essential to understand various factors controlling oxygen conditions at thermocline depths and its consequences on climate and marine life on various time scales.

The preservation of pteropod tests has been proved to be a potential proxy for reconstruction of past changes in thermocline ventilation, carbonate (aragonite) saturation depth and intermediate water circulation (Haddad & Droxler, 1996; Reichart *et al.*, 1998; Gerhardt & Henrich, 2001; Klöcker & Henrich, 2006; Singh *et al.*, 2005, 2006, 2011a, b; Singh, 2007; Böning & Bard, 2009; Singh & Singh, 2010; Sijinkumar *et al.*, 2010; Naidu *et al.*, 2014; Singh *et al.*, 2017). Pteropods, holoplanktic microgastropods are common members of microfaunal assemblages in Quaternary sediments of the Arabian Sea margins and topographic highs (e.g., Herman, 1971; Singh & Rajarama, 1997; Singh, 1998; Singh *et al.*, 2001, 2005; Singh & Singh, 2010; Singh *et al.*, 2011a, 2011b). Pteropod test being aragonitic in composition is susceptible to dissolution (Berner, 1976, 1977; Berger, 1978) and its preservation in sediment is related to the physico–chemical conditions of the water column (e.g., Almogi–Labin *et al.*, 1991, 1998; Reichart *et al.*, 1998; Gerhardt *et al.*, 2000; Klöcker *et al.*, 2006; Singh, 1998; Singh *et al.*, 2006; Singh, 2007). Aragonite being one of the metastable polymorphs of calcium carbonate is more prone to dissolution than calcite. The preservation of pteropod tests in sea–floor sediment depends on the aragonite compensation depth (ACD). Present day, the ACD in the Arabian Sea OMZ is shallow (~ 500 m), because the seawater in the OMZ is undersaturated with respect to aragonite due to high consumption of oxygen and poor ventilation of thermocline waters. Thus, the preservation record of fossil pteropod assemblage can reveal the signature of past variations in surface and subsurface water mass carbonate chemistry. Previous studies showed that the past changes in productivity, intermediate (thermocline) water ventilation and the depth of local overturning have resulted a significant variation in the OMZ intensity and the ACD (Altabet *et al.*, 1995; Reichart *et al.*, 1998; Klöcker *et al.*, 2006; Singh *et al.*, 2006, 2011a, b; Singh, 2007; Böning & Bard, 2009; Naidu *et al.*, 2014; Singh *et al.*, 2015; Verma *et al.*, 2018). The strength of OMZ thus governs the ACD, below which pteropod tests are completely dissolved. Hence, records of pteropod abundance and preservation from Arabian Sea sediment cores can archive changes in the intensity of the OMZ and the ACD (Singh *et al.*, 2006; Singh, 2007; Singh *et al.*, 2017). Most of the earlier palaeoceanographic reconstructions based on the Quaternary pteropods came from the Red Sea, Mediterranean Sea, Persian Gulf and the western Arabian Sea (e.g., Almogi–Labin *et al.*, 1986, 1998; Reichart *et al.*, 1998; Ivanova, 1999; Klöcker *et al.*, 2006); recently records from the eastern Arabian Sea have been added (Singh, 1998, 2007; Singh *et al.*, 2006; 2011a, b; Naidu *et al.*, 2014; Singh *et al.*, 2017). A high resolution pteropod record from the eastern Arabian Sea showing centennial to millennial scale variations in abundance and shell preservation is presented. The pteropod proxy records are used to better understand basin–wide changes in thermocline ventilation, OMZ intensity and ACD in response to the global climatic perturbations.

REGIONAL SETTING

The monsoonal wind system produces pronounced seasonal and spatial patterns in surface ocean circulation, hydrography and biological productivity in the Arabian Sea (Wyrtki, 1973; Naidu *et al.*, 2014). In summer monsoon (June to September), southwesterly winds blowing along the Somali Coast generate large scale coastal upwelling in the western and northern Arabian Sea and weak upwelling along the Southwest Coast of India (Wyrtki, 1973; Banse, 1987). During this period, the South Equatorial Current intensifies, the northern branch of which forms the Somali Current as a part of anticyclonic southwest monsoon circulation.

During the winter monsoon (December to March), the wind pattern reverses and a cyclonic circulation develops causing weak, sporadic upwelling along the coasts of Pakistan and India (Bauer *et al.*, 1991). The cold dry northerly–northeasterly winter winds also induce a decrease in sea–surface temperature and increase in sea–surface salinity due to high evaporation (Madhupratap *et al.*, 1996). This results in convective mixing in the northern and northeastern Arabian Sea. The biological productivity in the western and northern Arabian Sea is very high in summer monsoon; whereas during winter monsoon, a moderate increase in productivity is observed in the northern and northeastern Arabian Sea. During

⟶

Fig. 1—(A) Map showing the location of core MD76–131 (white star; this study) and other core sites discussed in the text (SO90–137, yellow circle and NIOP905, white circle) in the Arabian Sea. White dotted contour marks the intensified oxygen minimum zone (ASOMZ). (B) Oxygen (µmol/kg, colour shading overlain by O_2 contours) depth (m) -latitude section and vertical structure of water masses in the eastern Arabian Sea (N–S cross section from 25 °N to 60 °S). Map source is Ocean Data View (ODV; Schlitzer, 2014) using data from World Ocean Atlas 2018 (Garcia *et al.*, 2018). ASOMZ= Arabian Sea Oxygen Minimum Zone, SAMW= Sub–Antarctic Mode Water, AAIW= Antarctic Intermediate Water, CPDW= Circumpolar Deep Water, NIDW= North Indian Deep Water and AABW = Antarctic Bottom Water.

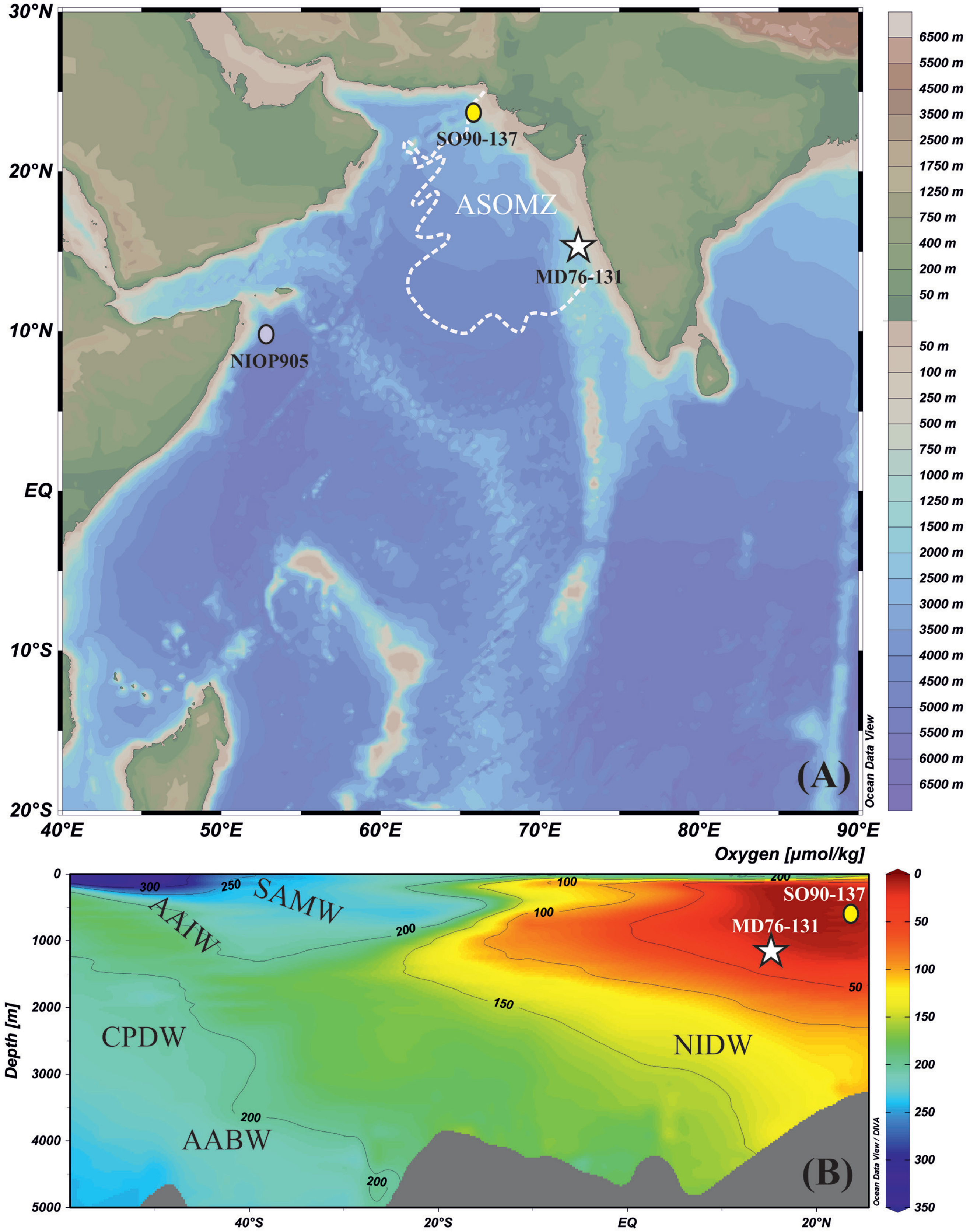
30°N
20°N
10°N
EQ
10°S
20°S
40°E
50°E
60°E
70°E
80°E
90°E
SO90-137
ASOMZ
MD76-131
NIOP905
(A)
Ocean Data View
6500 m
5500 m
4500 m
3500 m
2500 m
1750 m
1250 m
750 m
400 m
200 m
50 m
50 m
100 m
250 m
500 m
750 m
1000 m
1250 m
1500 m
2000 m
2500 m
3000 m
3500 m
4000 m
4500 m
5000 m
5500 m
6000 m
6500 m
Oxygen [µmol/kg]
Depth [m]
SAMW
AAIW
CPDW
AABW
NIDW
SO90-137
MD76-131
(B)
40°S
20°S
EQ
20°N
Ocean Data View / DIVA

the inter–monsoon periods, November to December and April to May, the entire Arabian Sea water column is stratified and characterized by nutrient–poor conditions.

The thermocline waters in the Arabian Sea are a combination of locally and externally generated water masses (Schott & McCreary, 2001). Two high–saline and O_2 poor water masses originate in the Persian Gulf (Persian Gulf Water: PGW) and the Red Sea (Red Sea Water: RSW) and flow into the Arabian Sea in a southeasterly direction at about 300 m and 500 m depth respectively (Schott & McCreary, 2001). However, the influence of PGW and RSW in the eastern Arabian Sea is less evident (Rameshbabu *et al.*, 1980). Southern sourced intermediate waters (Subantarctic Mode Water: SAMW and Antarctic Intermediate Water: AAIW) effectively ventilate the Arabian Sea thermocline (Olson *et al.*, 1993; You, 1998; Fine *et al.*, 2008) (Fig. 1). A complete reversal of the subsurface coastal circulation associated with the seasonal change in monsoon circulation also results in changes in oxygen–deficient waters of the eastern Arabian Sea (Naqvi, 1991). During the summer southwest monsoon, pole ward undercurrent carries well–oxygenated waters off the Indian margin. As monsoon wind reverses in winter, Arabian Sea high salinity waters flow equator ward. Thus, the renewal of the oxygen–deficient subsurface waters is more vigorous during the southwest monsoon than the northeast monsoon.

METHODOLOGY

Core location

A 9.65 m long piston core (MD76–131) was raised from central part of the western Indian margin at 1230 m water depth (off Goa: Lat. 15º 31.8' N; Long. 72º 34.1' E) by R/V *Marion Dufrense* in 1976 (Fig. 1). The core site is situated below the present day ACD (~ 500 m, Naidu *et al.*, 2014), but well above the Calcite Compensation Depth (~ 2400 m, Belyaeva & Burmistrova, 1984).

The sediment core in general is characterized by dark coloured indistinctly laminated sediments with intermittently light coloured homogenous facies. The narrow homogenous

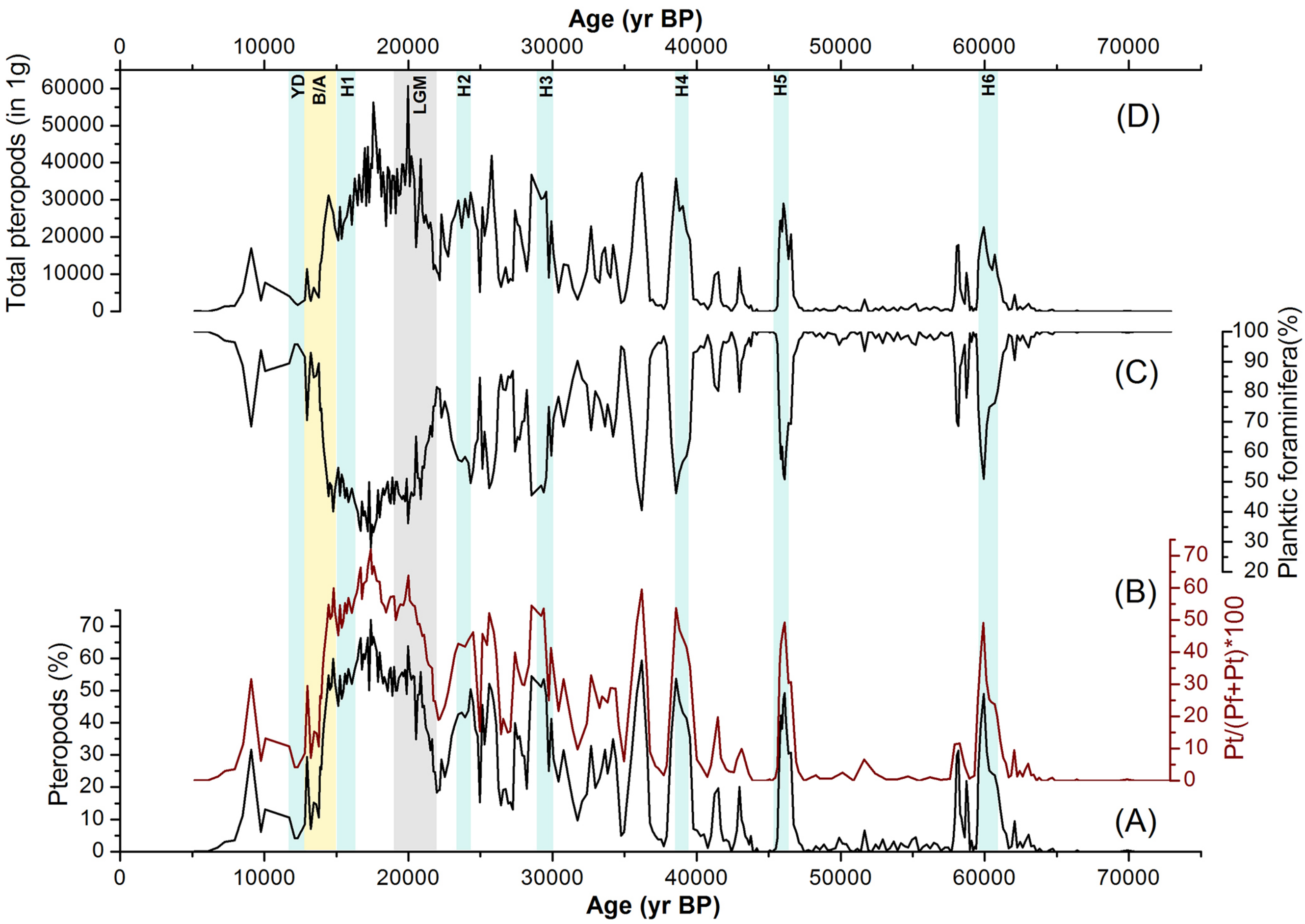

Fig. 2—Records of (A) relative abundance of pteropods, (B) ratio of pteropods to planktic foraminifera (Pt/(Pf+Pt)x100), (C) relative abundance of planktic foraminifera and (D) numerical abundance (g^{-1} dry sediment >125µm) of total pteropods in core MD76–131. Highlighted colour bands represent Heinrich Events (H1–H6, blue), Younger Dryas (YD, blue), Bølling/Allerød (B/A, yellow) and Last Glacial Maximum (LGM, grey).

intervals are lithologically in sharp contact with the laminated strata. The core provides uninterrupted sedimentary sequence (commonly hemi–pelagic mud), free of turbiditic (or mass flow) deposition and reworking (Singh *et al.*, 2006). The core was sampled at 1 to 2 cm intervals. Samples from 2 to 4 cm intervals were used for pteropod study.

Sample processing

For separation of pteropod tests, sediment samples were processed following conventional micropaleontological techniques (Singh *et al.*, 2005). About 5 g of dried sediment of each sample was wet sieved using a 63 µm screen. Dry residue larger than 63 µm was sieved again with a 125 µm screen. The coarse fraction (> 125 µm) was retained for pteropod analysis. For qualitative and quantitative analyses, the processed samples were sub–sampled using an Otto–Splitter to obtain suitable aliquots containing about 300 specimens of pteropod individuals. Those samples having less frequent pteropod tests were completely used for the separation of tests. Species identification, followed Van der Spoel (1967), Bé and Gilmer (1977), Van der Spoel and Boltovskoy (1981) and Singh *et al.* (2005).

Chronostratigraphy

The chronological framework of the core developed by Singh *et al.* (2011c) was adopted. The chronology of the core for 4 to 28 kyr BP is primarily based on 7 AMS radiocarbon ages. The calibration of radiocarbon ages to calendar ages was done with Calib 4.4 software package, after subtracting 640 years for reservoir corrections (Southon *et al.*, 2002). Beyond 30 kyr BP the chronostratigraphic control of the core was achieved by the correlation of $\delta^{15}N$ record of this core with stable oxygen isotope record of the GISP2 ice core (Singh *et al.*, 2011c). Age estimate of individual sample was

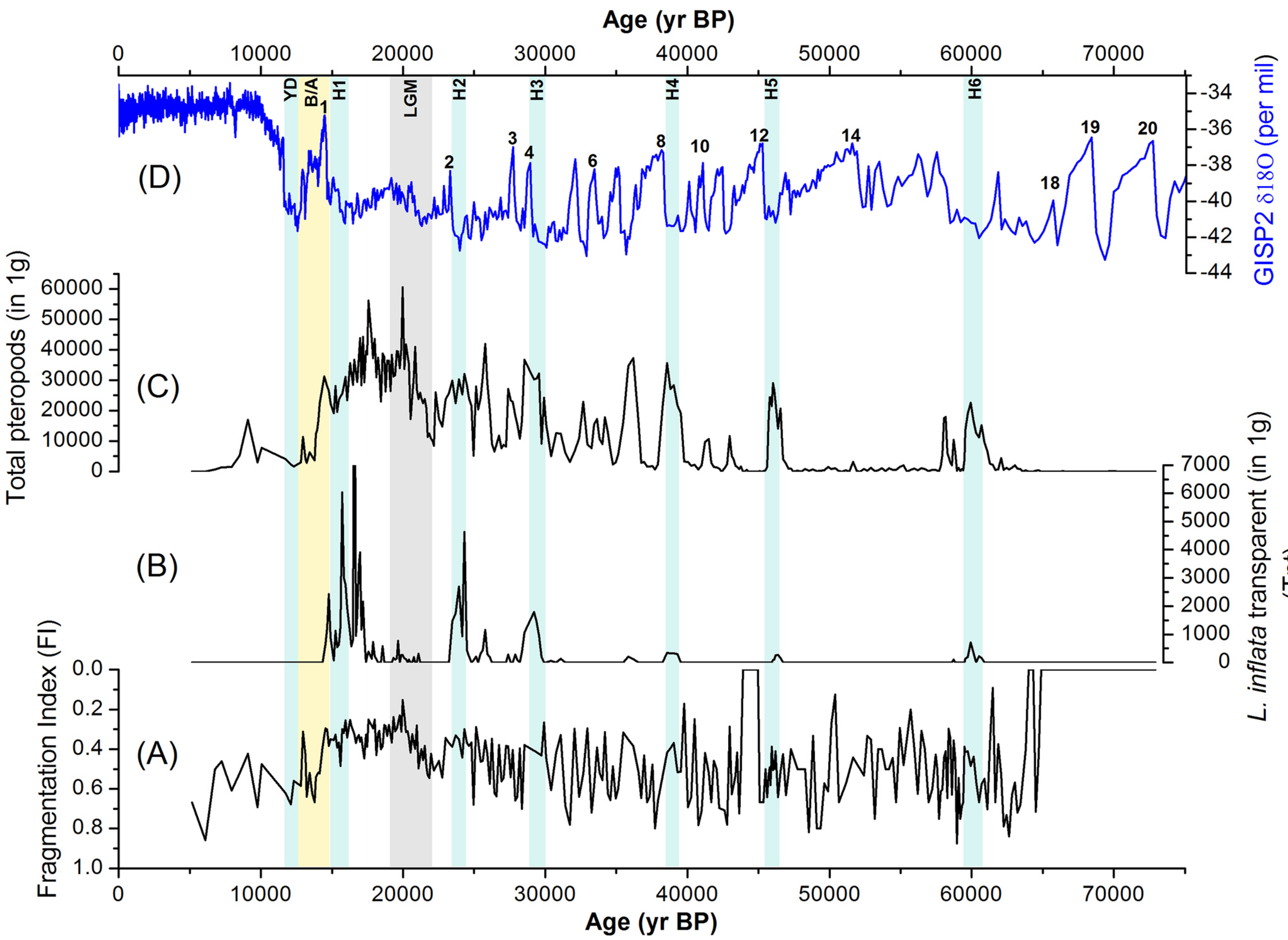

Fig. 3—Records of preservation indices and numerical abundance (g^{-1} dry sediment > 125 µm) of pteropods (this study) are compared with $\delta^{18}O$ record of GISP2 ice core (Stuiver & Grootes, 2000): (A) Fragmentation Index (FI: no. of pteropod fragments/whole tests and fragments), (B) numerical abundance of *Limacina inflata* transparent tests (Tpt), (C) numerical abundance of total pteropods and (D) GISP2 ice core $\delta^{18}O$. The numbers 1–20 in the GISP2 $\delta^{18}O$ record denote the D/O interstadials. Highlighted colour bands represent Heinrich Events (H1–H6, blue), Younger Dryas (YD, blue), Bølling/Allerød (B/A, yellow) and Last Glacial Maximum (LGM, grey).

calculated based on the linear interpolation between the age control points. A 70 kyr composite record of sediment shows an average sedimentation rate of ~13.85 cm kyr^{-1} at the core site. The linear sedimentation rates calculated between stratigraphic tie points range from ~7.06 cm kyr^{-1} (between 5 and 10 kyr BP) to ~26.71 cm kyr^{-1} (between 59 and 70 kyr BP). The high sedimentation rate with its average value of ~13.85 cm kyr^{-1} indicates that 1 cm thick sediment can provide a resolution of approximately ~70 years.

Pteropod proxies

Preservation indices—The processed samples contain complete and damaged pteropod tests and test fragments. We counted < 50 % damaged test as a whole pteropod test. All the fragments were also counted. The abundance of pteropods was estimated in 1 g of each sample. Based on the census data, the relative abundance (%) of each species was calculated. Aragonitic pteropods are more susceptible to the dissolution than the calcitic planktic foraminifera. In order to evaluate changes in the preservation of pteropod tests, the percentage of pteropods (Pt) relative to the sum of planktic foraminifera (Pf) and pteropods (Pt/(Pf + Pt)) was calculated as an index of the preservation/dissolution of aragonite (Almogi–Labin *et al.*, 1998; Singh, 2007).

Variations in the production rate can also influence the abundance of pteropod and foraminifera. To quantify this problem, we calculated a fragmentation index (FI=number of pteropod fragments/whole tests and fragments), a measurement independent of variable pteropod production. We took care to avoid mechanical damage of pteropod tests during processing of samples. However, a contribution of bottom currents in breaking these tests cannot be ruled out.

An additional reliable proxy for state of aragonite preservation is based on assessing the surface ultrastructure of certain pteropod species (Gerhardt *et al.*, 2000). The original test of a living pteropod is transparent. In the corrosive environment (in the water column and/or sediment) the transparent test alters into opaque–white and as dissolution progresses the test is damaged and ultimately dissolved (Haddad & Droxler, 1996). In this study, the state of fossil pteropod preservation was quantified based on the variation of transparent tests in population of *Limacina inflata*, a dissolution susceptible species (Singh *et al.*, 2006). The tests of *L. inflata* were grouped into two categories: (1) unaltered–transparent tests indicating good preservation and (2) altered–opaque white/damaged tests reflecting corrosion/dissolution.

RESULTS

The pteropod assemblages recovered from the sediments of core MD76–131 are characterized by low diversity and composed of both epipelagic and mesopelagic forms. *Limacina inflata* (d'Orbigny), *Limacina trochiformis* (d'Orbigny), *Creseis acicula* (Rang), *Creseis virgula* (Rang) forma *virgula* (Rang), *Creseis virgula* (Rang) forma *conica* (Eschscholtz), *Creseis chierchiae* (Boas), *Clio convexa* (Boas), *Clio pyramidata* (Linnaeus), *Cavolinia longirostris* (de Blainville), *Diacria quadridentata* (de Blainville) and *Styliola subula* (Quoy & Gaimard) are the common pteropod species. Other rare species are: *Dicaria trispinosa* (de Blainville), *Cavolinia gibbosa* (Rang), *Hyalocylix striata* (Rang) and *Limacina bulimoides* (d'Orbigny). Numerical abundance of the total pteropod tests (> 125 μm) in core samples is highly variable ranging from its complete absence to maximum up to 60638 /g. Pteropods are generally absent in the samples between 43.9 and 45.2 kyr BP and 63.6 and 72.9 kyr BP (Fig. 2). Intervals between 46.7 and 57.8 kyr BP and 5.1 and 7.9 kyr BP contain lowest abundance of pteropods (< 5000 specimens /g). Highest abundance of pteropod tests (> 20,000 specimens /g) occurs between 14.1 and 21.6 kyr BP (Fig. 2). Within this interval, there are two spikes of abundance maxima at 17.6 and 20 kyr BP. Other prominent peaks of pteropod abundances occur during 23–24.8 kyr BP, 25.1–26.1 kyr BP, 27.4 kyr BP, 28.5–29.6 kyr BP, 32.4–32.7 kyr BP, 35.5–36.5 kyr BP, 38.2–39.5 kyr BP, 45.7–46.6 kyr BP, and 59.5–60.7 kyr BP (Fig. 2). There are minor pteropod spikes occurring at 9 kyr BP, 13 kyr BP, 30.7–31.1 kyr BP, 33.5–34.4 kyr BP, 41.5 kyr BP, 43 kyr BP and 58 kyr BP. A chronology of pteropod abundance spikes identified in core MD76–131 is provided in Table 1. It is worth mentioning that most of the pteropod spikes occurring in MD76–131 correspond to the Northern Hemisphere cold Heinrich events (H1–H6) and Greenland stadials (Dansgaard–Oeschger events) (Fig. 3; Table 1) and some of these aragonite events are co–relatable with similar events reported from the western, northern and northeastern Arabian Sea records within the range of chronological error (Reichart *et al.*, 1998; Klöcker & Henrich, 2006; Klöcker *et al.*, 2006) (Fig. 5).

Planktic foraminifera (calcitic), which are more resistant to dissolution than pteropods (aragonitic), also show frequent variation in its abundance along the core. The numerical relation of these two pelagic groups (% Pteropod [Pt] / Planktic foraminifera [Pf] + Pteropod) is used as the indicator of the dissolution/preservation condition with respect to the aragonitic (pteropod) tests (Berner, 1977; Almogi–Labin *et al.*, 1998). Record of % Pt /Pf + Pt parallels the pteropod numerical abundance curve with high values corresponding to the abundance spikes (Fig. 2). A value (% Pt/Pf +Pt) of 50 % or more is found during 14.4–20.4 kyr BP, 25.1–26.1 kyr BP, 28.5–29.4 kyr BP, 35.8–36.2 kyr BP and 38.6–39.5 kyr BP. The abundance ratios of pteropods to planktic foraminifera are also high but < 50 % during other intervals of high pteropod abundance (45.7–46.6 kyr BP and 59.5–60.7 kyr BP). The pattern of fragmentation index (FI) clearly displays that pteropod abundance spikes correspond to the low values of FI (Fig. 3). However, this opposite relationship is not much evident for the interval of pteropod maximum during

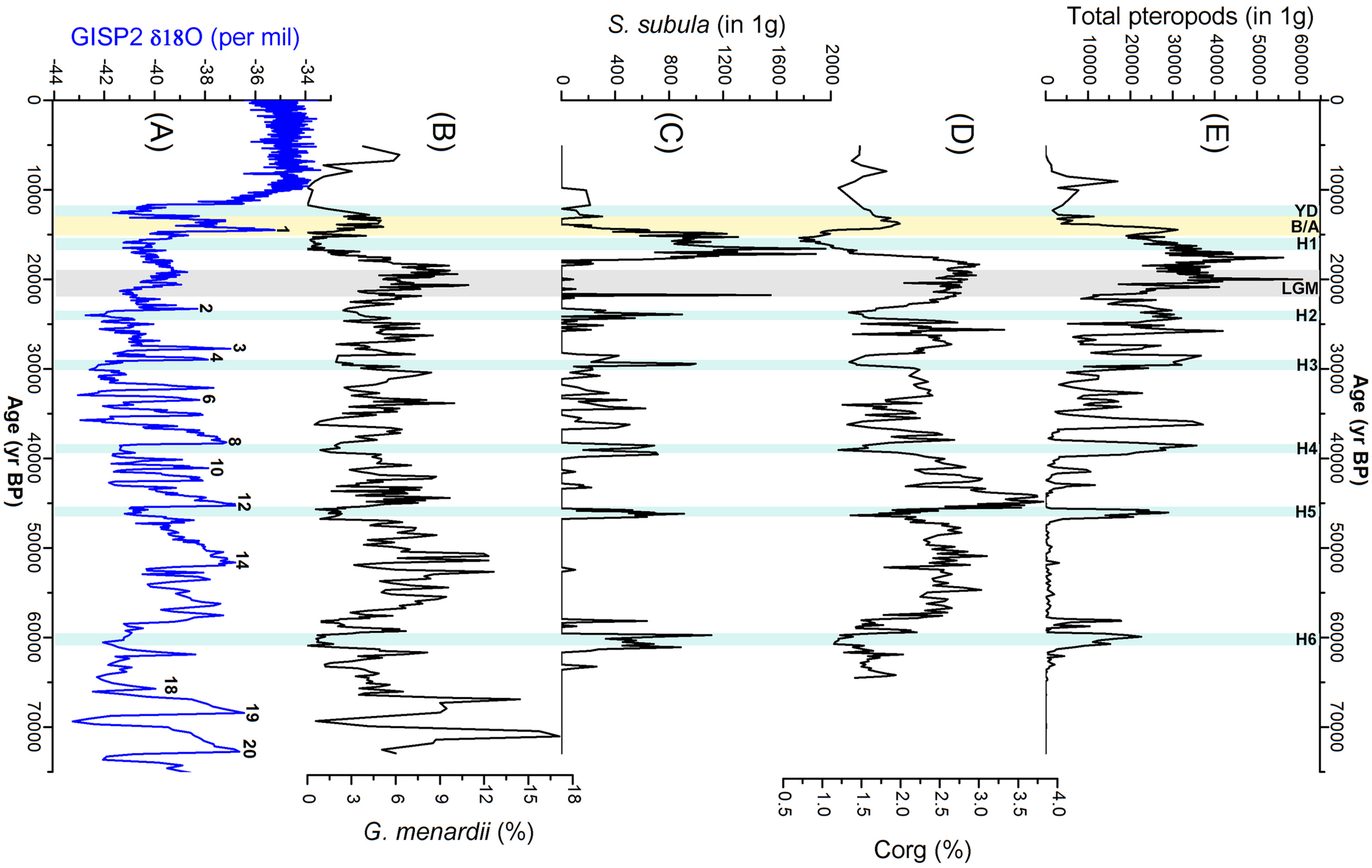

Fig. 4—Records of faunal proxies for dissolved oxygen in thermocline waters (*Globorotalia menardii*, *Styliola subula*) and numerical abundance (g^{-1} dry sediment > 125 µm) of total pteropods (this study) are compared with primary productivity record (Corg %) of core MD76–131 (Singh *et al.*, 2011c) and GISP2 ice core $\delta^{18}O$ record (Stuiver & Grootes, 2000): (A) GISP2 ice core $\delta^{18}O$, (B) % *Globorotalia menardii*, (C) numerical abundance of *Styliola subula*, (D) Corg % and (E) numerical abundance of total pteropods. The numbers 1–20 in the GISP2 $\delta^{18}O$ record denote the D/O interstadials. Highlighted colour bands represent Heinrich Events (H1–H6, blue), Younger Dryas (YD, blue), Bølling/Allerød (B/A, yellow) and Last Glacial Maximum (LGM, grey).

Table 1—High resolution record of Pteropod Events in the eastern Arabian Sea (MD76–131). Bold and blue lettered events are major Northern hemisphere climatic events (Heinrich events 1–6). The stadials are identified by comparison of pteropod preservation event chronology with the INTIMATE event stratigraphy, Rasmussen *et al.* (2014).

Preservation Event (Age)	Pteropod Abundance	Fragmentation Index (FI)	*L. inflata* Transparent Tests (Tpt)	Northern Hemisphere Climatic Events
9 kyr BP	Low	Medium	Absent	–
13 kyr BP	Low	Low	Absent	Stadial 1
14.3–15 kyr BP	High	Low	Low	–
15–17.3 kyr BP	High	Low	High	**Heinrich Event 1**
17.5–20.6 kyr BP	High	Low	Low	Stadial 2
23.5–24.5 kyr BP	Medium	Low	High	**Heinrich Event 2**
25.5–26.1 kyr BP	Medium	Low	Low	–
27.4 kyr BP	Medium	Low	Low	Stadial 3
28.5–29.6 kyr BP	Medium	Low	High	**Heinrich Event 3**
30.7–31.1 kyr BP	Low	Low	Low	Stadial 5
32.4–32.7 kyr BP	Medium	High	Absent	Stadial 6
33.5–34.4 kyr BP	Medium	Medium	Absent	Stadial 7
35.8–36.2 kyr BP	Medium	Low	Low	Stadial 8
38.6–39.3 kyr BP	Medium	Low	Low	**Heinrich Event 4**
41.5 kyr BP	Low	Medium	Absent	Stadial 10
43 kyr BP	Low	Low	Absent	Stadial 11
45.7–46.6 kyr BP	Medium	Medium	Low	**Heinrich Event 5**
58 kyr BP	Low	Medium	Absent	Stadial 16
59.5–60.7 kyr BP	Medium	Medium	Low	**Heinrich Event 6**

45.7–46.6 kyr BP. The interval between 14.4 and 20.6 kyr BP characterized by lowest average FI value suggests minimal natural breakage of pteropod tests, thus good preservation condition. Highest value of FI reported during 5–6 kyr BP indicates worse preservation of aragonitic tests (Fig. 3). The pteropod test preservation record (no. of transparent *L. inflata* tests, (Tpt)) reveals that the *L. inflata* population consists of significant number of least altered transparent tests during 15–17.5 kyr BP, 23.5–24.8 kyr BP and 28.4–29.6 kyr BP (Fig. 3). There are a few intervals where traces of transparent *L. inflata* tests are also found (25.1–26.1 kyr BP, 35.5–36.5 kyr BP, 38.2–39.5 kyr BP, 45.7–46.6 kyr BP and 59.5–60.7 kyr BP). These correspond to the spikes in pteropod abundance (Fig. 3). Otherwise the *L. inflata* population is characterized wholly by opaque–white tests.

DISCUSSION

The tests of the pteropod are preserved in sediments, when in situ CO_3^{2-}concentration exceeds the saturation concentration with respect to the aragonite. The mineral aragonite, a metastable polymorph of $CaCO_3$ is more soluble in seawater (by a factor of 1.5, Morse *et al.*, 1980) and dissolves at shallower depths than calcite. Today, the Arabian Sea is characterized by a pronounced OMZ basin–wide at water depths between 150 and 1250 m (Wyrtki, 1973) (Fig. 1). The sea water in the OMZ is undersaturated with respect to aragonite because of high consumption of oxygen and CO_2 addition due to oxidative destruction of organic matter which lowers the pH and carbonate saturation (Canfield & Raiswell, 1991). Because of a persistent sub–surface oxygen depleted condition resulting from the combined effects of high primary productivity, large flux of organic matter and poor ventilation of thermocline waters, the ACD in the eastern Arabian Sea is much shallower (~ 500 m) than other parts of the Arabian Sea (Singh, 2007). Therefore, the variation patterns of abundance and modes of preservation of pteropods in the core MD76–131 should be related to the changes in the ACD controlled by the OMZ strength which might have varied in the past due to fluctuations in the primary productivity and ventilation condition of thermocline waters.

Pteropod preservation events and patterns of monsoon induced productivity

Records of pteropod preservation indices (Tpt and FI) follow the pattern of pteropod abundance variation. Hence, the abundance spikes of pteropod tests are related to better state of aragonite preservation rather than variation in pteropod production. However, the preservation condition had changed through time, as evidenced from the quantitative variation of transparent tests in *L. inflata* population (Tpt) and values of relative abundance ratio of pteropod fragments and whole tests (fragmentation index, FI). Based on the high resolution abundance and preservation proxy data, we identified four stages of pteropod events characterizing a particular state of preservation condition. Pteropod event I (14.4–17.3 kyr BP) characterized by the high abundance of pteropod tests, low values of FI and maximum of transparent *L. inflata* tests relates to the best state of preservation. Pteropod event II (23.5–24.5 kyr BP, 28.5–29.6 kyr BP) represents a condition, when pteropods tests are better preserved but not as good as in case of pteropod event I. Pteropod event III (25.5–26.1 kyr BP, 35.8–36.2 kyr BP, 38.6–39.3 kyr BP, 45.7–46.6 kyr BP, 59.5–60.7 kyr BP) associated with less abundant transparent *L. inflata* tests and low to medium values of FI suggesting good preservation condition but poorer than event II. Pteropod event IV (9 kyr BP, 13 kyr BP,14.3–15 kyr BP, 17.5–20.6 kyr BP, 27.4 kyr BP, 30.7–31.1 kyr BP, 33.5–34.4 kyr BP, 41.5 kyr BP, 43 kyr BP, 58 kyr BP) represents an interval with devoid of transparent tests and medium values of FI. The intermittent intervals occurring between these pteropod preservation events are generally characterized by the absence of pteropod tests and fragments, which suggest a stage of severe aragonite dissolution. A comparison of our pteropod preservation record with the Greenland ice core temperature record indicate that the pteropod (aragonite) preservation spikes apparently correspond to the Northern Hemisphere cold events (Dansgaard–Oeschger (D–O) stadials and Heinrich events). The preservation of pteropods was poor during the warm phases of D–O cycles (interstadials). The ACD in the Arabian Sea, above which pteropod tests get preserved in sediments, is closely linked with the dissolved oxygen concentration in thermocline waters or in other words the strength of the OMZ (e.g., Reichart *et al.*, 1998). The surface ocean productivity has been considered as one of the main factors causing variation in the OMZ intensity and as a consequence the ACD (von Rad & Schulz, 1995; Singh *et al.*, 2006). We compared our pteropod preservation record with the primary productivity proxy record (Corg %) of core MD76–131 (Singh *et al.*, 2011c). There is a striking anti–correlation between pteropod preservation and Corg %. Low values of Corg % during the stadials and Heinrich events correlate very well with the pteropod preservation events. On the contrary, the warm interstadials are characterized by high Corg % and substantial or complete dissolution of pteropods (Fig. 4). Previous studies from this region have shown low productivity during Northern Hemisphere cold events (Heinrich events and stadials) linked to the weakening of both southwest (SW) summer and northeast (NE) winter monsoon circulations (Singh *et al.*, 2006, 2011c, 2018). Whereas, the SW monsoon induced productivity increased during the warm interstadials of the late glacial period. High export flux of organic matter and its decomposition leads to an increase of CO_2 concentration in thermocline waters, which lowers the pH resulting dissolution of aragonitic pteropod tests, OMZ intensification and shallowing of ACD. In contrast, when export flux of organic matter reduced during low productivity periods, the pteropod tests are well preserved because of higher pH in thermocline waters, deepening of ACD and a weak OMZ. Hence, the pteropod preservation in the eastern Arabian Sea is associated with the oxygenated thermocline waters during the periods of reduced productivity. Abundant occurrence of high oxygen–benthic foraminifera during the periods corresponding to the pteropod spikes further suggests an oxygenated benthic environment resulted due to the weakening of OMZ (Singh *et al.*, 2015; Verma *et al.*, 2018).

The pteropod preservation record from the eastern Arabian Sea is in agreement with the preservation records from the northern, northeastern and western Arabian Sea, which show pteropod preservation events occurring basin–wide during the cold stadials attributed to the low monsoon induced productivity, a weak OMZ and the deep ACD (e.g., Reichart *et al.*, 1998, 2002; von Rad *et al.*, 1999; Klöcker & Henrich, 2006; Klöcker *et al.*, 2006) (Fig. 5). It has also been suggested by a few workers (e.g., Reichart *et al.*, 1998; von Rad *et al.*, 1999) that intensified northeasterly winter monsoon winds during cold periods resulted deep vertical mixing of oxygen–rich waters, which enhanced the pH of thermocline waters and lowered the ACD in the northeastern Arabian Sea. Our record from the eastern Arabian Sea, however, does not support this hypothesis, as previous results of our study showed weakening of winter monsoon circulation during the cold stadials (Singh *et al.*, 2011c, 2018). Nevertheless, a large increase in pteropod abundance during the last glacial maximum (LGM) between 17.6 and 21.6 kyr BP is intriguing as this is associated with high Corg % (Fig. 4). Therefore, high oxygen condition within the thermocline cannot be explained by the productivity factor. There are several line of evidences suggesting intensification of the NE winter monsoon winds during the LGM (e.g., Reichart *et al.*, 1998; Singh *et al.*, 2006, 2011c, 2018). It is plausible that the strong winter winds might have resulted subduction of oxygen–rich surface waters into the thermocline through deep vertical mixing leading to a weak OMZ and deeper ACD. But this process does not seem to be applicable to the present area of investigation, because, we don't record pteropod preservation during the LGM in the core at shallower depth (SK 17; w. d. 840 m) (Singh *et al.*, 2006; Singh, 2007). Therefore, we argue for the factor other than winter mixing responsible for the thermocline ventilation

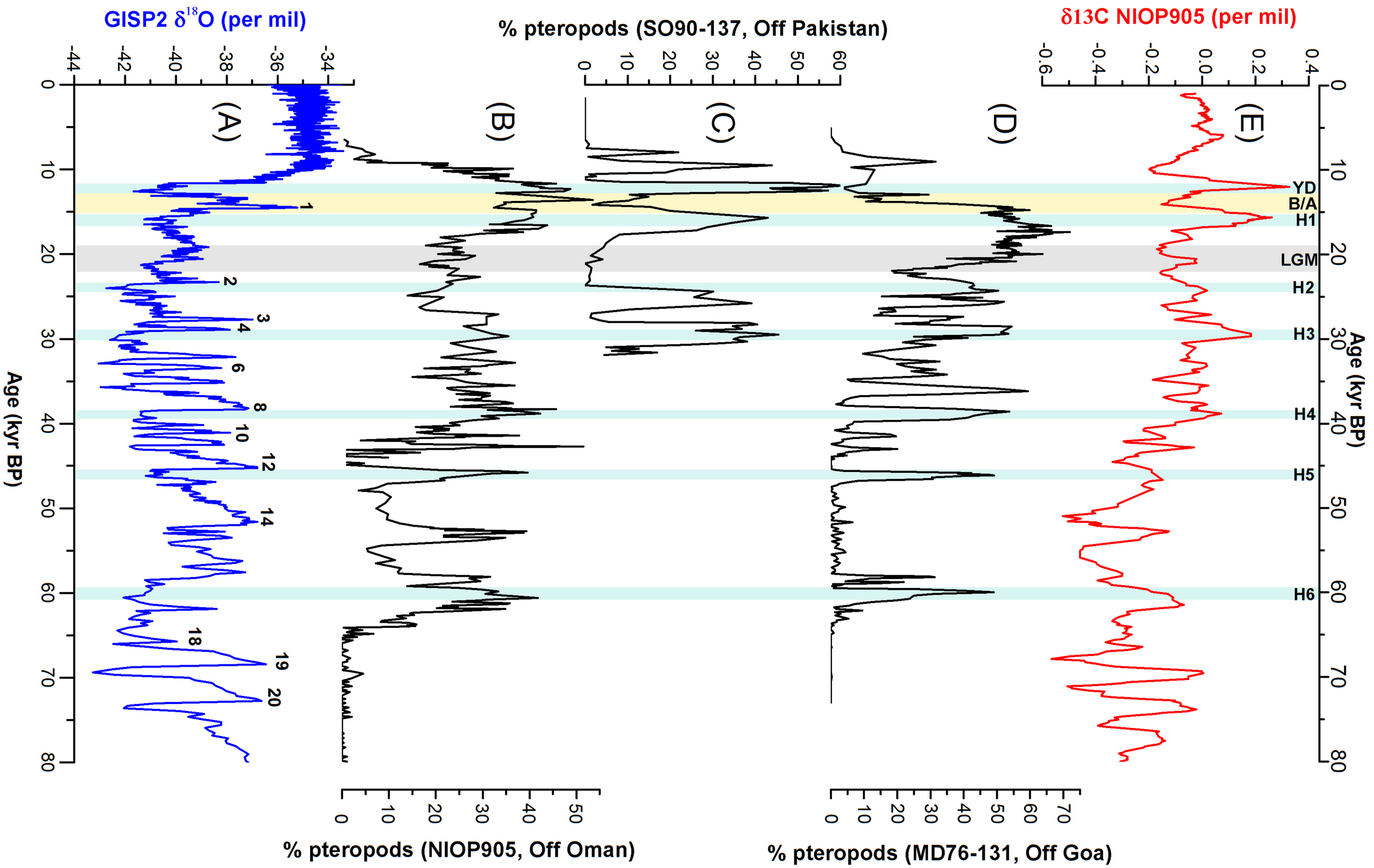

Fig. 5—Comparison of relative abundance of total pteropod records from the western (NIOP905, Klöcker *et al.*, 2006), northeastern (SO90–137, Klöcker & Henrich, 2006) and eastern Arabian Sea (MD 76–131, this study) with benthic foraminifera $\delta^{13}C$ record of western Arabian Sea (NIOP905, Jung *et al.*, 2009) and GISP2 ice core $\delta^{18}O$ record (Stuiver & Grootes, 2000): (A) GISP2 ice core $\delta^{18}O$, (B) % pteropods (NIOP905, Off Oman), (C) % pteropods (SO90–137, Off Pakistan), (D) % pteropods (MD76–131, Off Goa) and (E) benthic $\delta^{13}C$ (NIOP905). The numbers 1–20 in the GISP2 $\delta^{18}O$ record denote the D/O interstadials. Highlighted colour bands represent Heinrich Events (H1–H6, blue), Younger Dryas (YD, blue), Bølling/Allerød (B/A, yellow) and Last Glacial Maximum (LGM, grey).

and deepening of the OMZ during the LGM. However, with the present data set it is not possible to answer this question.

Thermocline ventilation and intermediate water circulation

Changes in pteropod preservation conditions are closely linked with the fluctuations in dissolved oxygen level in thermocline waters. In recent years, there have been growing number of palaeoceanographic studies from the tropical Indian Ocean showing enhanced thermocline ventilation in the Arabian Sea by externally sourced water masses in concert with the global climatic events (Kiefer *et al.*, 2006; Naidu & Govil, 2010; Mohtadi *et al.*, 2010; Visser *et al.*, 2003; Weldeab *et al.*, 2006; Jung *et al.*, 2009; Böning & Bard, 2009; Naidu *et al.*, 2014). Therefore, changes in thermocline circulation and its ventilation through time potentially modulate the OMZ intensity and the ACD and preservation of aragonitic pteropods. We used abundances of *Globorotalia menardii* (a thermocline planktic foraminifera) and *Styliola subula* (a mesopelagic pteropod) as proxies for dissolved oxygen levels in thermocline waters (Singh *et al.*, 2005, 2018; Naidu *et al.*, 2014). Singh *et al.* (2018) in their recent study from the eastern Arabian Sea have shown that *G. menardii* abundance significantly declines when oxygen levels in thermocline increased. High abundance of *S. subula* indicates oxygen–rich thermocline waters and a weak OMZ (Singh *et al.*, 2005). Both the proxy records show centennial to millennial scale changes pointing towards enriched dissolved oxygen levels in thermocline during the Northern Hemisphere cold events (stadials and Heinrich events), which correspond to the pteropod preservation spikes (Fig. 4). Intriguingly, we do not observe this pattern during the cold Younger Dryas event. Previous studies showed past changes in the Arabian Sea thermocline ventilation accompanied with remotely forced variations in the intensity of intermediate water circulations (e.g., Jung *et al.*, 2009; Böning & Bard, 2009). The thermocline water of the Arabian Sea has three possible sources: SAMW–AAIW, IIW and PGW–RSW (Böning & Bard, 2009). The two high density water masses (RSW and PGW) flowing into the Arabian Sea have little influence today in its eastern sector (Rameshbabu *et al.*, 1980). Palaeoceanographic records from the northeastern and western Arabian Sea provided evidence for strengthened influx of oxygen rich SAMW–AAIW to the Arabian Sea at thermocline depths during the cold Heinrich events and D–O stadials (Böning & Bard, 2009; Jung *et al.*, 2009). The oxygen replenishment of thermocline waters in the eastern Arabian Sea with the southern–sourced AAIW during the Northern Hemisphere cold events have been suggested by recent studies (Naidu *et al.*, 2014; Singh *et al.*, 2015). A significant reduction in Atlantic Meridional Overturning Circulation (AMOC) and North Atlantic Deep Water (NADW) during the cold stadials probably triggered the intensification of AAIW and its northward expansion (Pahnke & Zahn, 2005). Low oxygen demand because of reduced organic carbon flux combined with high oxygen supply by intensified thermocline circulation during the cold stadials led to the deepening of ACD and high preservation of pteropod tests. On the contrary, high organic flux and poorly ventilated thermocline during the warm interstadials resulted in shallow ACD and poor pteropod preservation.

The pteropod abundance records from the western and northeastern Arabian Sea show an overall agreement with the eastern Arabian Sea record indicating basin–wide abundance maxima during the Heinrich events (Fig. 5). Jung *et al.* (2009) based the benthic $\delta^{13}C$ record from the western Arabian Sea suggested increased incursion of southern sourced waters ventilating the thermocline during cold Heinrich and Younger Dryas events. However, our pteropod abundance and preservation proxy records along with thermocline oxygen proxies (*G. menardii* and *S. subula*) do not suggest a significant ventilation of thermocline waters in the eastern Arabian Sea during the Younger Dryas. A pronounced increase in pteropod abundance as recorded in northeastern Arabian Sea during the Younger Dryas and Heinrich 1 and 2 might also be related to the intensified winter monsoon wind induced vertical mixing, which would have brought oxygen–rich surface waters down deep into the thermocline (e.g., Reichart *et al.*, 1998; Schulte & Müller, 2001). The pteropod abundance maxima recorded in the eastern and northeastern Arabian Sea during the early Holocene at around 9 kyr BP is intriguing and that can't be explained with the present data.

This study highlights how changes in global oceanic circulation modulated oxygen condition of thermocline waters in the Arabian Sea, the OMZ and ACD in response to the abrupt climate changes at centennial to millennial scales. However, relative contributions of different deep water masses including Arabian Sea Deep Water, North Atlantic Intermediate Water, Indonesian Throughflow Water in ventilating Arabian Sea thermocline both in time and space still remain poorly understood. Therefore, further work on foraminifera (stable C and O isotopes, Nd isotopes and trace elements) is needed to address this issue.

Acknowledgements*—I thank Vandana Prasad and Binita Phartiyal for inviting to contribute in Special Issue of the Journal of Palaeosciences. This research was supported by IoE incentive grant of Banaras Hindu University. I also thank Harshit Singh for preparation of figures and formatting of the manuscript.*

REFERENCES

Almogi–Labin A, Hemleben C & Meischner D 1998. Carbonate preservation and climate changes in the central Red Sea during the last 380 ka as recorded by the pteropods. Marine Micropaleontology 33: 87–107.

Almogi–Labin A, Hemleben C, Meischner D & Erlenkeuser H 1991. Paleoenvironmental events during the last 13,000 years in the central Red Sea as recorded by pteropoda. Paleoceanography 6: 83–98.

Almogi–Labin A, Luz B & Duplessy JC 1986. Quaternary paleoceanography, pteropod preservation and stable isotope record of the Red Sea. Palaeogeography, Palaeoclimatology, Palaeoecology 57: 195–211.

Altabet MA, Francois D, Murray W & Prell WL 1995. Climate–related variations in denitrification in the Arabian Sea from 15N/14N ratios. Nature 373: 506–509.

Altabet M, Higginson M & Murray D 2002. The effect of millennial–scale changes in Arabian Sea denitrification on atmospheric CO_2. Nature 415: 159–162. https://doi.org/10.1038/415159a

Banse K 1987. Seasonality of phytoplankton chlorophyll in the central and northern Arabian sea. Deep Sea Research Part A. Oceanographic Research Papers 34: 713–723.

Bauer S, Hitchcock GL & Olson DB 1991. Influence of monsoonally–forced Ekman dynamics upon surface layer depth and plankton biomass distribution in the Arabian Sea. Deep Sea Research Part A. Oceanographic Research Papers 38(5): 531–553. https://doi.org/10.1016/0198–0149(91)90062–K

Bé AWH & Gilmer RW 1977. A zoogeographic and taxonomic review of euthecosomatous Pteropoda. *In:* Ramsay ATS (Editor)—Oceanic Micropalaeontology, Academic Press, London 1: 733–808.

Belyaeva NV & Burmistrova II 1984. Foraminiferal lysocline and critical levels of carbonate sedimentation in the Indian Ocean. Litologiya i Poleznye Iskopaemye, Russian 6: 57–66.

Berger WH 1978. Deep–sea carbonate: Pteropod distribution and aragonite compensation depth. Deep Sea Research 25: 447–452.

Berner RA 1977. Sedimentation and dissolution of pteropods in the oceans. In: Andersen NR & Malahoff A (Editors)–The fate of fossil fuel CO_2 in the Oceans, Plenum Press, New York: 243–260.

Berner RA 1976. The solubility of calcite and aragonite in seawater at atmospheric pressure and 34.5 % salinity. American Journal of Science 276: 713–730.

Böning P & Bard E 2009. Millennial/centennial–scale thermocline ventilation changes in the Indian Ocean as reflected by aragonite preservation and geochemical variations in Arabian Sea sediments. Geochimica et Cosmochimica Acta 73: 6771–6788.

Canfield DE & Raiswell R 1991. Carbonate precipitation and dissolution. *In:* Allison PA & Briggs DEG (Editors)—Taphonomy: releasing the data locked in the fossil record, Plenum Press, New York: 411–453.

Feely RA, Sabine CL, Lee K, Berelson W, Kleypas J, Fabry VJ & Millero FJ 2004. Impact of anthropogenic CO_2 on the $CaCO_3$ system in the oceans. Science 305: 362–366.

Fine RA, William MS Jr, John LB, Monika R, Dong–Ha M, Mark JW, Alain P & Ray FW 2008. Decadal ventilation and mixing of Indian Ocean waters. Deep–Sea Research Part I 55: 20–37. https://doi.org/10.1016/j.dsr.2007.10.002

Garcia HE, Weathers K, Paver CR, Smolyar I, Boyer TP, Locarnini RA, Zweng MM, Mishonov AV, Baranova OK, Seidov D & Reagan JR 2018. World Ocean Atlas 2018, Volume 3: Dissolved Oxygen, Apparent Oxygen Utilization, and Oxygen Saturation. A. Mishonov Technical Ed.; NOAA Atlas NESDIS 83: 38pp.

Gerhardt S, Groth H, Ruhlemann C & Henrich R 2000. Aragonite preservation in late Quaternary sediment cores on the Brazilian continental slope: implications for intermediate water circulation. International Journal of Earth Sciences 88: 607–618.

Gerhardt S & Henrich R 2001. Shell preservation of *Limacina inflata* (Pteropoda) in surface sediments from the Central and South Atlantic Ocean: A new proxy to determine the aragonite saturation state of water masses. Deep Sea Research, Part I 48(9): 2051–2071.

Haddad GA & Droxler AW 1996. Metastable $CaCO_3$ dissolution at intermediate water depths of the Caribbean and western North Atlantic: Implications for intermediate water circulation during the past 200,000 years. Paleoceanography 11: 701–716.

Herman Y 1971. Vertical and horizontal distribution of pteropods in Quaternary sequences. *In:* Funnell BM & Reidel WR (Editors)–The Micropalaeontology of Oceans, Cambridge University Press, Cambridge: 463–486.

Ivanova EM 1999. Late Quaternary monsoon history and paleoproductivity of the western Arabian Sea. Ph. D thesis, Free University, Netherlands.

Jung SJA, Kroon D, Ganssen G, Peeters F & Ganeshram RS 2009. Enhanced Arabian Sea intermediate water flow during glacial North Atlantic cold phases. Earth and Planetary Science Letters 280: 220–228.

Keeling RF & Garcia H 2002. The change in oceanic O_2 inventory associated with recent global warming. Proceedings of the National Academy of Sciences 99(12): 7848–7853.

Kiefer T, McCave IN & Elderfield H 2006. Antarctic control on tropical Indian Ocean sea surface temperature and hydrography. Geophysical Research Letters 33: L24612. doi: 10.1029/2006GL027097

Klöcker R & Henrich R 2006. Recent and Late Quaternary pteropod preservation on the Pakistan shelf and continental slope. Marine Geology 231(1–4): 103–111.

Klöcker R, Ganssen G, Jung SJA, Kroon D & Henrich R 2006. Late Quaternary millennial–scale variability in pelagic aragonite preservation off Somalia. Marine Micropaleontology 59: 171–183.

Madhupratap M, Kumar S, Bhattathiri P, Kumar M, Raghukumar S, Nair K & Ramaiah N 1996. Mechanism of the biological response to winter cooling in the northeastern Arabian Sea. Nature 384: 549–52. doi: 10.1038/384549a0

Mohtadi M, Steinke S, Luckge A, Groeneveld J & Hathorne EC 2010. Glacial to Holocene surface hydrography of the tropical eastern Indian Ocean. Earth and Planetary Science Letters 292: 89–97.

Morse JW, Mucci A & Millero FJ 1980. The solubility of calcite and aragonite in seawater at various salinities, temperatures and atmosphere total pressure. Geochimica et Cosmochimica Acta 44: 85–94.

Naidu PD, Singh AD, Ganeshram RS & Bharti SK 2014. Abrupt climate–induced changes in carbonate burial in the Arabian Sea: Causes and consequences. Geochemistry, Geophysics, Geosystems 15(1): 1398–1406. https://doi.org/10.1002/2013GC005065

Naidu PD & Govil P 2010. New evidence on the sequence of deglacial warming in the tropical Indian Ocean. Journal of Quaternary Sciences 25: 1138–1143. https://doi.org/10.1002/jqs.1392

Naqvi SWA 1991. Geographical extent of denitrification in the Arabian Sea in relation to some physical processes. Oceanologica Acta 14: 281–290.

Olson DB, Hitchcock GL, Fine RA & Warren BA 1993. Maintenance of the low–oxygen layer in the central Arabian Sea. Deep Sea Research Part II: Topical Studies in Oceanography 40: 673–685.

Orr JC, Fabry VJ, Aumont O, Bopp L, Doney SC, Feely RA, Gnanadesikan A, Gruber N, Ishida A, Joos F & Key RM 2005. Anthropogenic ocean acidification over the twenty–first century and its impact on calcifying organisms. Nature 437: 681–686.

Pahnke K & Zahn R 2005. Southern Hemisphere water mass conversion linked with North Atlantic climate variability. Science 307(5716): 1741–1746. https://doi.org/10.1126/science.1102163

Rameshbabu V, Varkey MJ, Kesava Das V & Gouveia AD 1980. Water masses and general hydrography along the west coast of India during early March. Indian of Journal Marine Sciences 9: 982–989.

Rasmussen SO, Bigler M, Blockley SP, Blunier T, Buchar SL, Clausen HB, Cvijanovic I, Dahl–Jensen D, Johnsen SJ, Fischer H, Gkinis V, Guillevic M, Hoek WZ, Lowe J, Pedro JB, Popp T, Seierstad IK, Steffensen JP, Stevensson AP, Vallelonga P, Vinther BM, Walker MJC, Wheatley JJ & Winstrup M 2014. A stratigraphic framework for abrupt climate changes during the last glacial period based on three synchronized Greenland ice–core records: refining and extending the INTIMATE event stratigraphy. Quaternary Science Reviews 106: 14–28.

Reichart GJ, Schenau SJ, De Lange GJ & Zachariasse WJ 2002. Synchroneity of oxygen minimum zone intensity on the Oman and Pakistan Margins at sub–Milankovitch time scales. Marine Geology 185: 403–415.

Reichart GJ, Lourens LJ & Zachariasse WJ 1998. Temporal variability in the northern Arabian Sea oxygen minimum zone (OMZ) during the last 225000 years. Paleoceanography 13: 607–621.

Riebesell U, Zondervan I, Rost B, Tortell PD, Zeebe RE & Morel FMM 2000. Reduced calcification of marine plankton in response to increased atmospheric CO_2. Nature 407: 364–367.

Sabine CL, Feely RA, Gruber N, Key RM, Lee K, Bullister JL, Wanninkhof R, Wong CS, Wallace DWR, Tilbrook B, Millero FJ, Peng TH, Kozyr A, Ono T & Rios AF 2004. The oceanic sink for anthropogenic CO_2. Science 305: 367–371. DOI: 10.1126/science.1097403

Schlitzer R 2014. Ocean Data View. http://odv.awi.de

Schott F & McCreary JP 2001. The monsoon circulation of the Indian Ocean. Progress in Oceanography 51: 1–123.

Schulte S & Müller PJ 2001. Variations of sea surface temperature and primary productivity during Heinrich and Dansgaard-Oeschger events in the northeastern Arabian Sea. Geo–Marine Letters 21: 168–175.

Schulz H, Von Rad UV & Erlenkeuser H 1998. Correlations between Arabian Sea and Greenland climate oscillations of the past 110,000 years. Nature 393: 54–57.

Sijinkumar AV, Nath BN & Guptha MVS 2010. Late Quaternary record of pteropod preservation from the Andaman Sea. Marine Geology 275: 221–229.

Singh AD & Rajarama KN 1997. Distribution of pteropods in surface sediments from the continental shelf of north Kerala. Journal of the Geological Society of India 49: 81–84.

Singh AD 1998. Late Quaternary oceanographic changes in the eastern Arabian Sea: Evidence from planktonic foraminifera and pteropods. Journal of Geological Society of India 52: 203–212.

Singh AD, Ramachandran KK, Samusuddin M, Nisha NR & Haneeshkumar V 2001. Significance of pteropods in deciphering the Late Quaternary sea–level history along the south western Indian shelf. Geo–Marine Letters 20: 243–251.

Singh AD, Nisha NR & Joydas TV 2005. Distribution patterns of recent pteropods in surface sediments of the western continental shelf of India. Micropaleontology 24: 39–54.

Singh AD, Kroon D & Ganeshram R 2006. Productivity and OMZ intensity variation in the eastern Arabian Sea at the millennial scale. Special issue on Holocene Indian Monsoon. Journal of Geological Society of India 68: 369–377.

Singh AD 2007. Episodic preservation of pteropods in the eastern Arabian Sea: Monsoonal change, oxygen minimum zone intensity and aragonite compensation depth. Indian Journal of Marine Science 36: 378–383.

Singh AD & Singh OP 2010. Potentiality of pteropods in reconstruction of the Quaternary climatic and oceanographic history of the Arabian Sea. Gondwana Geological Magazine 25(1): 81–88.

Singh AD, Das S & Verma K 2011a. Impact of climate induced hypoxia on calcifying biota in the Arabian Sea: an evaluation from the micropalaeontological records of the Indian margin. Mausam 62: 647–652.

Singh AD, Verma K & Singh OP 2011b. Carbonate preservation and monsoon wind induced hydrographic changes in the eastern Arabian Sea during the Last 30 kyr as recorded by pteropods. *In:* Singh DS & Chhabra NL (Editors)–Geological processes and climate change, MacMillan Publishers India Ltd, New Delhi, India: 1–8.

Singh AD, Jung SJA, Darling K, Ganeshram R, Ivanochko T & Kroon D 2011c. Productivity collapses in the Arabian Sea during glacial cold phases. Paleoceanography 26(3): PA3210. doi: 10.1029/2009PA001923

Singh AD, Rai AK, Verma K, Das S & Bharti SK 2015. Benthic foraminiferal diversity response to the climate induced changes in the eastern Arabian Sea oxygen minimum zone during the last 30 ka BP. Quaternary International 374: 118–125.

Singh AD, Jung SJA, Anand P, Kroon D & Ganeshram RS 2018. Rapid switch in monsoon–wind induced surface hydrographic conditions of the eastern Arabian Sea during the last deglaciation. Quaternary International 479: 3–11.

Singh DP, Saraswat R, Naik DK & Nigam R 2017. A first look at factors affecting aragonite compensation depth in the eastern Arabian Sea. Palaeogeography, Palaeoclimatology, Palaeoecology 483: 6–14. https://doi.org/10.1016/j.palaeo.2016.09.014

Southon J, Kashgarian M, Fontugne M, Metivier B & W–S Yim W 2002. Marine reservoir corrections for the Indian Ocean and Southeast Asia. Radiocarbon 44: 167–180.

Stramma L, Johnson GC, Sprintall J & Mohrholz V 2008. Expanding oxygen–minimum zones in the tropical oceans. Science 320(5876): 655–658. doi: 10.1126/science.1153847.

Stuiver M & Grootes PM 2000. GISP2 Oxygen isotope ratios. Quaternary Research 53: 277–284. https://doi.org/10.1006/qres.2000.2127

Van der Spoel S & Boltovskoy D 1981. Pteropoda. *In:* Boltovskoy D (Editor)—Atlas del zooplancton del Atlánticosudoccidental y métodos de trabajo con el zooplankton marino, Publicación Especial, Instituto Nacional de Investigación y Desarrollo Pesquero, Mar del Plata: 493–531.

Van der Spoel S 1967. Euthecosomata, a group with remarkable developmental stages (Gastropoda, Pteropoda), J. Noorduijn.en Zoon NV, Gorinchem. [Ph. D. Thesis, University of Amsterdam]: 375 pp.

Verma K, Bharti SK & Singh AD 2018. Late Glacial–Holocene record of benthic foraminiferal morphogroups from the eastern Arabian Sea OMZ: Paleoenvironmental implications. Journal of Earth System Science 127: 21–35. https://doi.org/10.1007/s12040–018–0920–9

Visser K, Thunell R & Stott L 2003. Magnitude and timing of temperature change in the Indo–Pacific warm pool during deglaciation. Nature 421: 152–155.

Von Rad U & Schulz H 1995. Sampling the oxygen minimum zone off Pakistan: glacial–inter–glacial variations of anoxia and productivity (preliminary results). Marine Geology 124: 7–19.

Von Rad U, Schulz H, Riech V, den Dulk M, Berner U & Sirocko F 1999. Multiple monsoon–controlled breakdown of oxygen–minimum conditions during the past 30,000 years documented in laminated sediments off Pakistan. Palaeogeography, Palaeoclimatology, Palaeoecology 152(1–2): 129–161.

Weldeab S, Schneider RR & Kölling M 2006. Deglacial sea surface temperature and salinity increase in the western tropical Atlantic in synchrony with high latitude climate instabilities. Earth and Planetary Science Letters 241(3): 699–706. https://doi.org/10.1016/j.epsl.2005.11.012

Wyrtki K 1973. Physical oceanography of the Indian Ocean. *In:* Zeitzschel B & Gerlach SA (Editors)—the Biology of the Indian Ocean, Springer, New York: 18–36.

You Y 1998. Intermediate water circulation and ventilation of the Indian Ocean derived from water-mass contributions. Journal of Marine Research 56(5): 1029–1067. https://doi.org/10.1357/002224098765173455